EXPERIMENTAL STUDY AND SIMULATION ON DISPLACEMENT OF SOFT DIELECTRIC ELASTOMER ACTUATORS

İbrahim KARAMAN [1], Davut Erdem ŞAHİN [2]

[1] Yozgat Bozok Üniversitesi, Mechatronics Engineering Department, 66100, Yozgat, Turkey
[2] Yozgat Bozok Üniversitesi, Mechanical Engineering Departman, 66100, Yozgat, Turkey
Corresponding author: İbrahim KARAMAN, E-mail: ibrahim.karaman@yobu.edu.tr
[1] ORCID iD: https://orcid.org/0000-0001-8396-9797; [2] ORCID iD: https://orcid.org/0000-0001-6770-7252

Abstract. Dielectric elastomer (DE) is a type of polymer that provides deformation by applying electrical voltage. There are many factors that affect the performance of DE, such as voltage, pre-stretching, frequency type applied, and frequency size. In this study, displacement changes with time resulting from the applied voltages in a circular dielectric elastomer actuator (DEA) were first determined experimentally, and then predicted numerically. In order to reveal the deformation behavior of DEA quantitatively, two significant factors, such as voltage and frequency were considered in the scope of this study. Experimental results showed that both voltage and frequency play a very important role in the displacement of DEA. Numerical predictions and experimental measurements found in this study provides in-depth information to researchers for controlling the deformation behavior of DEA depending on the arranging of these two key parameters. The attained results were elucidated that the deformation behavior of DEA is considerably influenced by the frequency type and frequency amplitude. The numerical analysis was implemented utilizing the Yeoh hyperelastic material model in commercial finite element code Abaqus. The experimental outcomes were favorably compared to the numerical predictions. It was found that the square waveform causes the faster and higher displacement in DEA in comparison with other waveforms including triangle and sine. Furthermore, it was observed that an increase in pre-stretching leads to an enhancement in the deformation of DEA. Nevertheless, experiencing the breakdowns by DEA experiences at very high voltages was revealed.

Key words: soft robotic, dielectric elastomer actuators, displacement, Yeoh, frequencies.

1. INTRODUCTION

In recent years, those working in materials science have been investigating electroactive polymers (EAP) as a promising material for a new actuator technology. Dielectric elastomers (DEs), a subcategory of EAPs, have promising properties as new smart materials that can convert electrical energy into mechanical energy [1]. Compared to electroactive ceramics and shape memory alloys, DEs have advantages such as fast response, low noise, and large deformations. DE material possesses many great advantages over conventional electromagnetic systems [6, 7]. DEAs are widely used as components in many devices such as artificial muscles, soft robots, photonic devices, and energy harvesters [2–5]. Generally, Dielectric Elastomer Actuators (DEAs) consist of a thin dielectric elastomer membrane between two compatible electrodes. Pelrine et al. [6, 9] reported that DE takes place at a high voltage and high speed, and the DEA sustains large strains higher than 100%. Figure 1 shows the working principle of DEA. When a voltage is applied to the DE film, the film expands in the planar direction and the elastomer thickness decreases [8]. Depending on the voltage, electrical charges of opposite poles accumulate on the two faces of the membrane, which results in reducing its thickness, and therefore expanding its area. Voltage causes shape change and DE behaves like an actuator [10–13]. A voltage applied to the DE leads to a mechanical reaction. Since the structure of DEA is similar to a structure of living muscle, it can also be used as a sensor [14–16]. In particular, actuators that convert an applied electric field into mechanical motion are used in many robotic applications, including biomimetic robots, prostheses, and artificial muscles [3, 17].

In these applications, the electrical energy resulting from the deformation is converted into mechanical energy [18]. The electrostatic pressure taken place in the DEA due to the deformation is called the Maxwell stress and it is defined by the following expression.

$$p = \varepsilon_r \varepsilon_0 E^2 = \varepsilon_r \varepsilon_0 (V/d)^2. \tag{1}$$

In this equation, ε_r is the dielectric constant, ε_0 is the free space permittivity ($8.85\times10\text{-}12$ F / m), E is the electric field, V is the voltage, p is the Maxwell stress, d is the elastomer thickness.
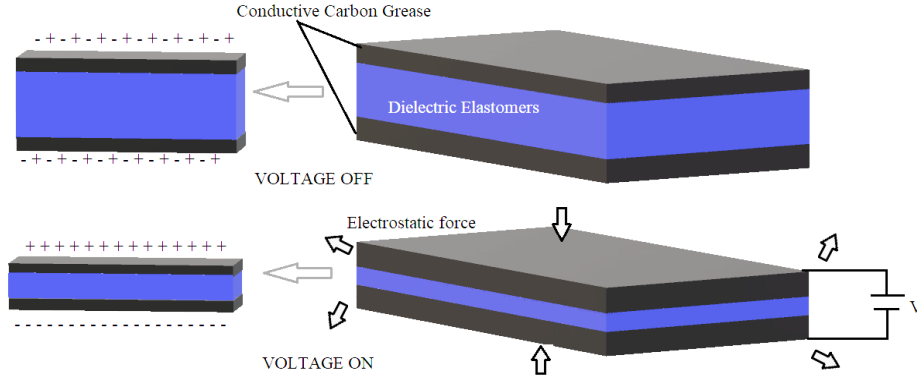

Fig. 1 – Working principle of dielectric elastomer actuator.

The DE membrane is sandwiched between the two electrodes as depicted in Fig. 1. Electrodes consist of a soft material possessing lower mechanical hardness than elastomer. Carbon grease is usually used for electrodes because of their good conductivity. The charges of opposite poles on these two electrodes cause the membrane (DE) to deform. The voltage applied to the DE results in substantial stretching of the DE. Since DEAs have similar properties to natural muscles, such soft actuators are often used to develop biomimetic soft robots such as worm robots, human-like robots, and robotic fish [19, 20]. When the operating frequencies are examined in the literature, DEA deformation decreases as the frequency increases, and in the same manner, the deformation in DEA decreases at very low frequencies [21, 22, 36]. The best mechanical reaction for circular DEAs is attained by the applied voltage at different frequencies ranging from 0.2 Hz to 10 Hz [23, 36]. Hyperelastic materials are used in many industries. The most important properties of hyper elastic materials, such as rubber are their capability of undergoing large deformations without failure. These types of materials exhibit highly non-linear deformation behavior under loads [24, 25]. The geometric dimensions of DEA are defined as $l_1 \times l_2 \times l_3$, and the stretch ratios in all directions are defined as $\lambda_1 = l_1/L_1$, $\lambda_2 = l_2/L_2$ and $\lambda_3 = l_3/L_3$. Here, l_1, l_2 and l_3 are the three main constants, in addition, λ_1, λ_2 and λ_3 are the principal stretch ratios. In the theory of rubber elasticity, there are several well-tested functions for strain-energy density depending on the deformation of the elastomer, for example neo-Hookean, Mooney-Rivlin, Yeoh, Gent, Ogden and Arruda-Boyce. In this research, experiments are simulated using the Yeoh model. An analytical method has been developed to study the elongation of a circular DEA using the Yeoh model. As a result of the deformation analyzed in Abaqus, the Yeoh model in biaxial simple shear provides a stable analytical description of the material stress-strain response and a good agreement between numerical and experimental data even at large stress values [26]. The Yeoh hyperelastic material model is a reduced third-order polynomial model used for the deformation of nearly incompressible, nonlinear elastic materials such as rubber. The strain-energy density (or stored energy density) in polynomial form for a compressible rubber can be given as [27]:

$$W = \sum_{i=1}^{3} C_{i0} \left(\bar{I}_1 - 3\right)^i + \sum_{i=1}^{3} \frac{1}{D_i} \left(J_l - 1\right)^{2i}. \tag{2}$$

Here, W represents the strain energy per unit of reference volume. Furthermore, C_{i0} and D_i denote the temperature-dependent material parameters. Moreover, $\bar{I}_1$ is the first deviatoric strain invariant and it can be defined as $\bar{I}_1 = \bar{\lambda}_1^2 + \bar{\lambda}_2^2 + \bar{\lambda}_3^2$. Where, the deviatoric stretches $\bar{\lambda}_i = J^{-\frac{1}{3}} \lambda_i$. Herein, J represents the total

volume change, in addition, λ_i denotes the principle stretches. Furthermore, the initial shear and bulk modulus can be defined as $\mu_0 = 2C_{10}$ and $K_0 = \dfrac{2}{D_1}$, respectively.

In 1993, Yeoh proposed a third-order polynomial phenomenological model based solely on the first invariant $l1$. It can be used for the characterization of carbon black filled rubber and can capture the elevation of the stress-strain curve. It is compatible with a wide range of stresses and can simulate various deformation modes with limited data. This leads the requirements of materials testing to be reduced [28]. In this experimental study, the displacement of DEAs as a result of their reaction to electrical signals and voltage has been investigated.

From the experiments conducted in this study, it has been revealed that the square waveform in electrical signals is displaced more and faster in a short time. Also, it has been found that the displacement increases with increasing voltage. Furthermore, it has been observed that DEs are damaged when high voltage is applied (over 5kV). The square waveform gives the best response for the time dependent displacement. It is seen that DEAs work effectively at applied voltage between 3kV and 5kV. Time-dependent displacement of DEAs have been recorded with a camera, and experimental results have been obtained. In addition, numerical analysis of the experiments has been implemented in Abaqus/Standard 3D finite element engineering code. It has been concluded that the Yeoh model used in the simulations provides a good agreement compared to the experimental results.

2. MATERIAL AND METHODS

2.1. Mathematical model

Changes in DEA thickness and carbon grease area affect the electric field, and thus the Maxwell stress. Since the disruptive input could not be measured, the voltage source and the desired voltage of the equipment have been assumed to be constant during the measurement process. In this case, the system makes a free oscillating motion. In the second stage, the system has been driven by different electrical signals such as square, triangle and sine. In this case, besides the undesired fluctuations specified in the first case, the movement of the system has been determined by AC signals. In this case, the system makes a harmonic motion. Since the disruptive input could not be measured, the system has been under dynamic condition rather than static conditions. Additionally, the voltage source and the desired voltage of the equipment have been assumed to be constant during the process.

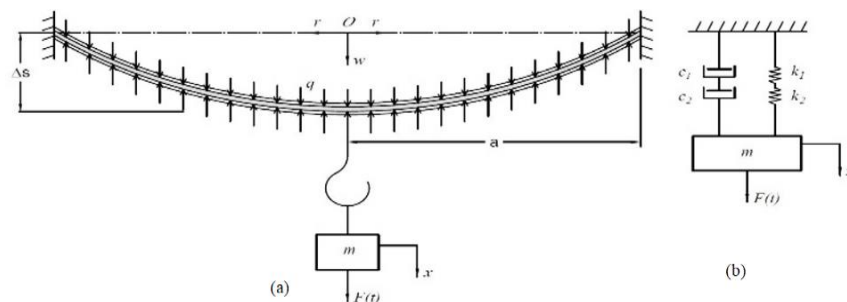The mathematical representation of the DEA system is shown in Fig. 2.

Fig. 2 – Mathematical model of DEA: a) reel system; b) equivalent system.

Herein, Δs and *q represent* a *static displacement* and a *uniformly distributed load*, respectively. Furthermore, k_1 and k_2 *are the equivalent stiffnesses,* and c_1 and c_2 *denote the equivalent damping coefficients*. Since the stretch in the hook is negligible compared to the elastomer, it can be written that $x = w$ and $k_{eq}=k_1$, $c_{eq}=c_1$ by *neglecting the effects of c_2 and k_2 parameters on the system*. Based on this, the equation of motion of the system can be defined in discrete form by the following expression

$$m_{eq}\ddot{x} + c_{eq}\dot{x} + k_{eq} = F(t) \, . \tag{3}$$

$F(t)$ in Eq. (3) can be determined by the set of equations as follows:

$$F(t) = \begin{cases} S_g(t)\left(\dfrac{\varepsilon_r \varepsilon_0}{d^2(t)}\right)V^2(t) & \text{for constant voltage} \\[4mm] S_g(t)\left(\dfrac{\varepsilon_r \varepsilon_0}{d^2(t)}\right)\left[\displaystyle\sum_{n=1}^{\infty} b_n \sin\left(\dfrac{2\pi n t}{T}\right)\right]^2 & \text{for sine wave} \\[4mm] S_g(t)\left(\dfrac{\varepsilon_r \varepsilon_0}{d^2(t)}\right)\left[\displaystyle\sum_{n=1}^{\infty} b_n \sin\left(\dfrac{2\pi n t}{T}\right)\right]^2 & \text{for square wave} \\[4mm] S_g(t)\left(\dfrac{\varepsilon_r \varepsilon_0}{d^2(t)}\right)\left[a_0 + \displaystyle\sum_{n=1}^{\infty} a_n \cos\left(\dfrac{2\pi n t}{T}\right)\right]^2 & \text{for triangle wave} \end{cases} \tag{4}$$

The system subjected to the constant voltage is under free vibration condition whereas the system excited by AC signals is under harmonically forced vibration condition. V is amplitude of electric voltage function $V(t)$, S_g – square of grafit on DEA surface, T – period of signals and a_0, a_n, b_n are Fourier coefficients documented in Table 1.

<div align="center">Table 1
Fourier coefficients of electrical signals</div>

Frequencies	a_0	a_n	b_n
Triangle	$\dfrac{V}{2}$	$\dfrac{-4V}{n^2\pi^2}$	
Square			$\dfrac{-3}{n\pi}\left[\cos(n\pi)-1\right]$
Sine	$\dfrac{2V}{\pi}$	$\dfrac{2V}{\pi(1-n^2)}$	$b_1 = \dfrac{V}{2}$

2.2. Design principle

DE materials consist of silicone, polyurethane, or acrylic. The most widely used DE material produced by 3M Company in the market is acrylic VHB4910 and VHB4905 tapes [29, 30]. These tapes are flexible materials with double-sided adhesion, sustaining high deformation under tension and high dielectric resistance [31]. In the literature, carbon grease, carbon powder and metallic fine wires are used due to its demanded adhesion property and being a good conductor [4, 31–33]. Carbon grease electrodes are the most popular choice because they are inexpensive and easy to apply in most dielectric elastomers with excellent adhesion. Dry graphite and carbon powder is easy to use, which is also inexpensive and easy to apply. They are more suitable for multi-layer DEAs than carbon grease electrodes because of their ease of application [34, 35].

In the experiments, a commercial VHB4910 manufactured by 3M company and a dc-dc converter (EMCO Q80-5) with an input voltage of 0~5 volts and capable of producing 8 kV and a generator with square, triangle, sine waveforms in the frequency range of 0.12Hz ~ 2MHz (tt t-echnic vc2002 function signal generator) was used . Carbon grease (846, MG Chemicals) selected as the electrode has been applied to both sides of the DE by brushing. The electrode-coated DE has been pre-stretched equally in both directions. The experimental setup to measure the displacement of DE under varying frequency and voltage is depicted in Fig. 3. As seen in Fig. 3, a mass of 46.22 g has been attached to the geometric center of the DEA. When the weight has been attached, the static deflection has been measured to be 2 mm. The diameter of DEA has been enhanced from 3.5 cm to 7 cm because of the applied pre-stretching. A perforated pad with a diameter of 1.5 cm has been mounted on the geometric center of DEA. For the purpose of using the carbon grease as the electrode, carbon grease was applied to both surfaces of DEA with the diameter of 3 cm. After the carbon grease was applied to both sides of the elastomer, the circuit was completed by connecting it to the dc-dc converter with copper adhesive tapes. In order to measure the total voltage applied to the DEA, 10 resistors were connected with each other in serial $(10\,\text{M}\Omega)$ and the total voltage was computed by

multiplying the measured voltage in one resistor by 10. Video recordings during the experiments were acquired by synchronizing the displacement stopwatch and the camera on the DEA as shown in Fig. 3. By examining the video recordings, time-dependent displacements were extracted and transferred to the computer environment. The thickness of the VHB4910 tape used in the experiments is 1 mm. On the DE, carbon grease was applied by brushing. Hence, the thickness of the carbon grease could not be detected exactly.

Fig. 3 – DEA experimental setup.

The finite element analysis of the conducted experiments was implemented using the commercial engineering code Abaqus/Standard 3D. The finite element modelling of the test is illustrated in Fig. 4. To define the material behavior of DE under load used in our experiments, hyperelastic material model developed by Yeoh was accounted for in our simulations. Yeoh hyperelastic material model parameters used in the simulations are tabulated in Table 2. The numerical analysis was performed in three various stages. In the first stage, the pre-stretching was dictated to the DE. In the second stage, the static instantaneous mechanical loading resulting from the mounted mass on the geometric center of the DE was applied to the pre-stretched DE. Albeit there are many material models developed for the mechanical characterization of the hyperelastic materials, Yeoh model with the constants obtained from the literature (Table 2) provided the most accurate predictions compared to the experimental results in terms of the static deflection. Thus, Yeoh model was preferred to utilize as the constitutive material model in our simulations. In the last stage, mechanical loads caused by the voltage imposed to the DE in different waveforms, like square, sine and triangular was applied to the DEA.

Table 2

Coefficients of Yeoh, Abaqus/Standard 3d form, material model [26]

C_{10} (MPa)	C_{20} (MPa)	C_{30} (MPa)	D_1	D_2	D_3
0.2019	$4.43e^{-5}$	$1.295e^{-4}$	$2.1839e^{-3}$	$8.68e^{-5}$	$-1.794e^{-5}$

Shell element formulation was used in numerical analysis. The waveforms accounted for in our simulations are shown in Fig. 5.
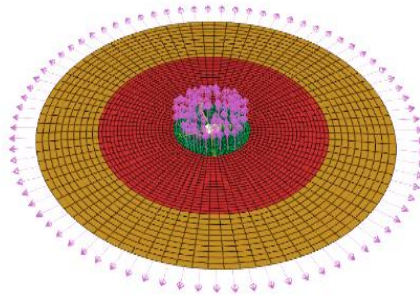

Fig. 4 – Finite element model of dielectric elastomers subjected to waves in different forms.

In electrical signals, the amplitude of the wave at a time of t is one of the most important factors affecting the deformation of DEA. When the amplitude is increased in the square waveform, mechanical elongation takes place more in DEA because a linear electrical signal is obtained. Here, the amplitude of the sine waveform gives the amplitude of the wave along a line in the equation $k = \omega/c = 2\pi f/c = 2\pi/\lambda$, with λ – wavelength, c – propagation velocity and f – frequency. The applied voltage $V(t) = V\sin(\omega t)$, frequency between 1 Hz and 20 Hz has been applied.
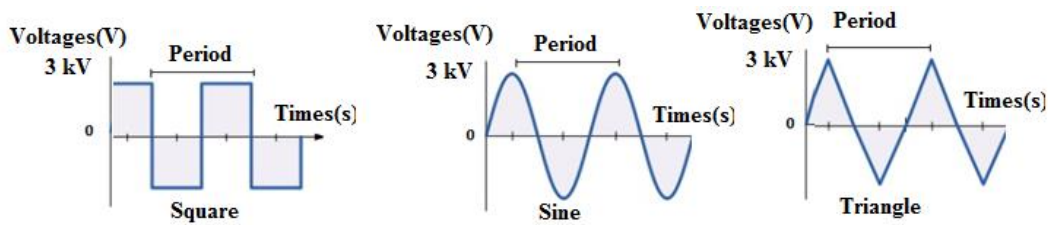

Fig. 5 – Different Electrical Signals Applied to DEA.

In the experiments, electrical signals were not applied consecutively. In other words, each electrical signal was applied alone. For instance, when the square waveform is applied, the point at which the displacement reaches its maximum value is taken into consideration. The high voltage source that is capable of increasing the input voltage from $0 \sim 5V$ to output voltage of $8\,kV$ was used to drive the DE actuator.

3. RESULTS

3.1. Displacement of DEA due to voltage

The displacement change in DEA caused by the applied voltage is experimentally measured and the experimental measurements are compared to the numerical calculations that are done by using the following parameters in MATLAB R2020a. Dielectric constant ($\varepsilon_r = 4.7$), free space permittivity ($\varepsilon_0 = 8.85 \times 10^{-12}$ F/m), strain limit (Jlim = 120) and strain-slip modulus 25.4 kPa for VHB4910 were taken into account for the calculations in MATLAB. The experimental results are compared to the numerical calculations as shown in Fig. 6. From the Fig. 6, it can readily be deduced that the deflection of DEA nonlinearly increases with increasing voltage. At high voltages higher than $5\,kV$, DEA loses its structural ability to deform because a catastrophic failure led by breakdowns is taken place in DEA. At low voltages, the elongation is less due to the low electromechanical loading on the DEA. With the consideration of Hooke's law, the elongation taken place in the DEA is computed by using the thickness stress equation in MATLAB.

$$sz = -p/Y = p = \varepsilon_r\,\varepsilon_0\,E^2 = \varepsilon_r\,\varepsilon_0\,(V/d)^2. \tag{5}$$

The stretch ratio can be written as $\lambda = \varepsilon_r\,\varepsilon_0/Y$. Here, sz is the thickness stress, p is the maxwell, Y is the Young's modulus, and d is the elastomer thickness. Due to the very fast response of the elastomer resulting from the applied tension, its time dependent displacement could not be determined.
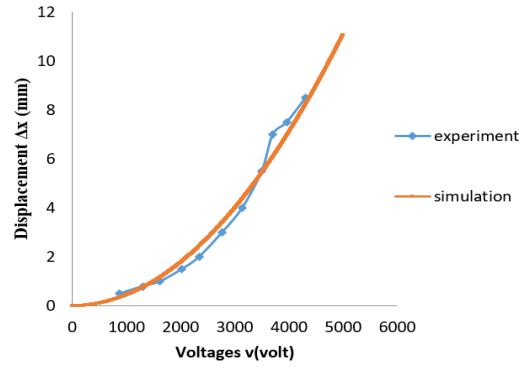
Fig. 6 – Displacement variation of dielectric elastomer subjected to direct form wave in experiment and simulation.

The displacement contour of the DEA for the applied voltage of 3 kV is depicted in Fig. 7. In terms of displacements, the experimental results are in a good agreement with the numerical predictions.
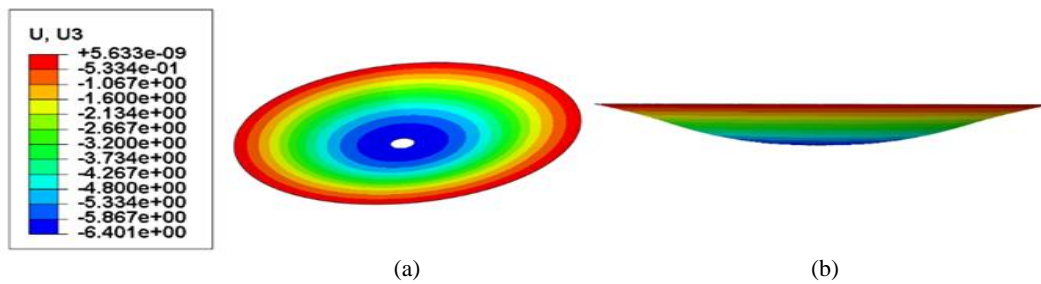

(a)   (b)

Fig. 7 – Displacement contour of dielectric elastomer subjected to direct form wave: a) isometric view; b) front view.

3.2. Displacement status over time at different frequencies applied to DEAs

Time-dependent displacement variations were investigated for the DEA that is subjected to the voltage of 3 kV at a broad range of frequency varying from 1 Hz to 20 Hz. The deflection change of DEA with time is illustrated in Fig. 8 for three various waveforms. Experimental results revealed that the square waveform leads to the larger displacement, in addition, the displacement reaches its maximum value with shorter time in the square waveform in comparison with the other waveforms. These findings can be comprehended from the results in Fig. 8. While the maximum displacement registered under the square waveform is 4 mm, the maximum displacements for other two waveforms are found to be 3 mm. It is seen that the displacement is variable when the system is forced by the alternating electric field. Therefore, the system needs to be considered as a dynamic problem. Since the designed DEA system is aimed to be used in artificial muscle applications, maximum displacement reached by the DEA was taken into account.
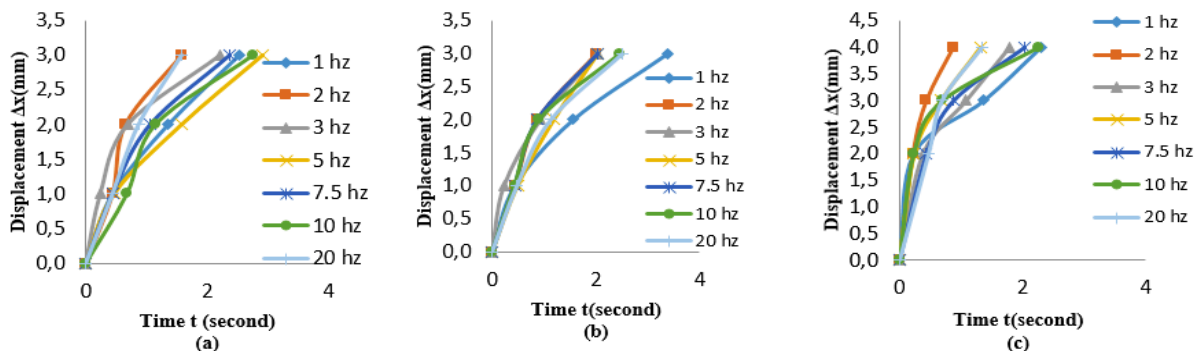

Fig. 8 – Displacement contour of dielectric elastomer subjected to: a) sine wave; b) triangle wave; c) square wave.

When the frequency ranges considered in our study are examined, the fastest reaction occurs at 2 Hz, as shown in Fig. 8. Compared to the triangle waveform, the obtained reaction time in sine waveform is shorter. The numerically predicted displacement contours of DEA for three various waveforms at 3 kV with

the frequency of 20 Hz are indicated in Fig. 9. As with the experimental results, the numerical analysis predicts the maximum displacement for the square waveform as well as illustrated in Fig. 9 and Fig. 12.
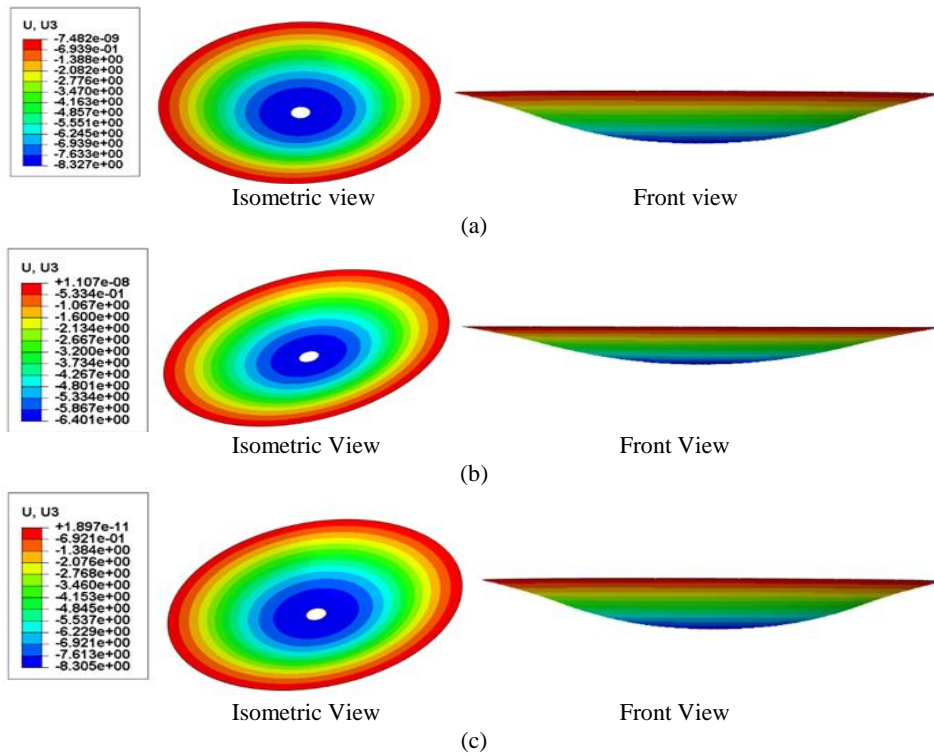

Fig. 9 – Displacement contour of dielectric elastomer subjected to: a) square form wave; b) triangular form wave; c) sine form wave applied 3 kV voltages and 20 Hz frequencies.

As can be comprehended from Fig. 10, the fastest response is attained in the square waveform with the frequency of 2 Hz at 3 kV voltage.
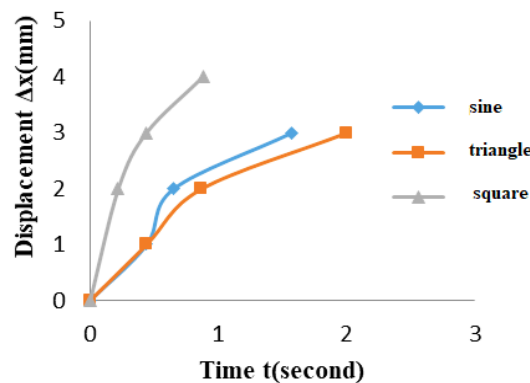

Fig. 10 – Displacement variation of dielectric elastomer subjected to waveforms under with 3 kV voltage 2 Hz frequencies.

Whereas the response of DEA is linear at low frequencies, the displacement reaches its maximum value in larger time at high frequencies. In sine and triangular waveforms, as the frequency approaches 1 kHz, the maximum displacement can only reach up to 1 mm as documented in Fig. 11. Additionally, there is no reaction taken place in DEA at frequencies higher than 1 kHz for both sine and triangle waveforms. In comparison with the triangular waveform, the reaction takes place in shorter time under sine waveform at high frequencies. In square waveform, on the other hand, above 10 kHz, the displacement of the DEA decreases, and the reaction time increases. It was determined that the square waveform responds faster with a higher displacement at high frequencies compared to the sine and triangular waveforms, as reported in Fig. 11.
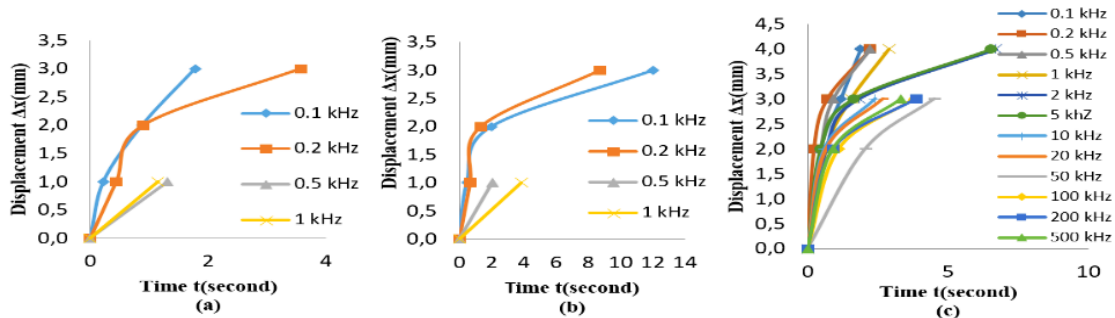
Fig. 11 – Displacement contour of dielectric elastomer subjected to: a) sine wave; b) triangle wave;
c) square wave under with 3 kV voltages and high frequencies.

Figure 12 shows the predicted displacement variation taken place in the DEA with time for three various waveforms under 3 kV voltage at 20 Hz, including square, triangle and sine.
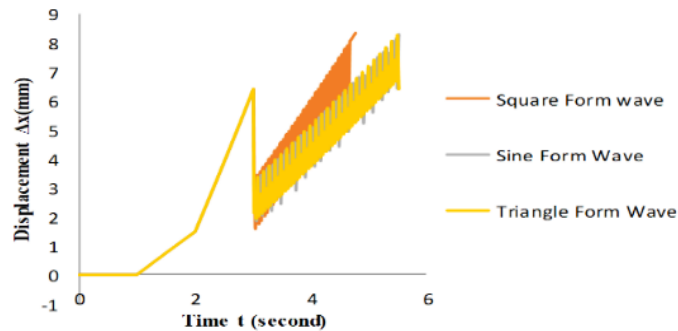

Fig. 12 – Displacement variation of dielectric elastomer with time subjected to different waveforms.

4. CONCLUSION

The following conclusions can be drawn from both experimental and numerical results as follows:

DEA deforms due to the thinning of the elastomer thickness as well as an increase in the electrostatic pressure on the DEA.

The most promising results in terms of displacement are found at voltages lying between 3kV and 5kV.

A type of electrical signal plays a considerable role in the reaction of DEA.

Compared to triangle and sine waveforms, the square waveform with the frequencies varying from 2 Hz and 10 Hz results in larger displacement in the DEA.

The experimental results show good agreements with the numerical predictions.

The displacements taken place in the DEA are found to be less at high frequencies (kHz).

This study is pioneering researchers to make a decision on selecting the most suitable waveform, frequency and voltage ranges for attaining the most efficient operating condition of DEA.

ACKNOWLEDGEMENTS

REFERENCES

1. Y. BAR-COHEN, *Artificial muscles based on electroactive polymers as an enabling tool in biomimetics*, Proceedings of the Institution of Mechanical Engineers, Part C: Journal of Mechanical Engineering Science, **221**, *10*, pp. 1149-1156, 2007.
2. K.J. KIM, S. TADOKORO, *Electroactive polymers for robotic applications*: *Artificial muscles and sensors*, Springer, 2007.
3. P. BROCHU, Q. PEI, *Dielectric elastomers for actuators and artificial muscles*, In: *Electroactivity in polymeric materials* (ed. L. Rasmussen), Springer, 2012, pp. 1-56.
4. P.I. GALICH, S. RUDYKH, *Shear wave propagation and band gaps in finitely deformed dielectric elastomer laminates: long wave estimates and exact solution*, Journal of Applied Mechanics, **84**, *9*, p. 091002, 2017.
5. R. GETZ, G. SHMUEL, *Band gap tunability in deformable dielectric composite plates*, International Journal of Solids and Structures, **128**, pp. 11-22, 2017.

6. R. PELRINE, R. KORNBLUH,, J. JOSEPH, R. HEYDT, Q. PEI, S. CHIBA, *High-field deformation of elastomeric dielectrics for actuators*, Materials Science and Engineering: C, **11**, *2*, pp. 89-100, 2000.
7. Q. PEI, R. PELRINE, S. STANFORD, R. KORNBLUH, M. ROSENTHAL, *Electroelastomer rolls and their application for biomimetic walking robots*, Synthetic Metals, **135**, pp. 129-131, 2003.
8. C. JEAN-MISTRAL, A. SYLVESTRE, S. BASROUR, J.J. CHAILLOUT, *Dielectric properties of polyacrylate thick films used in sensors and actuators*, Smart materials and structures, **19**, *7*, p. 075019, 2010.
9. R.E. PELRINE, R.D. KORNBLUH, J.P. JOSEPH, *Electrostriction of polymer dielectrics with compliant electrodes as a means of actuation*, Sensors and Actuators A: Physical, **64**, *1*, pp. 77-85, 1998.
10. R. PELRINE, R. KORNBLUH, Q. PEI, J. JOSEPH, *High-speed electrically actuated elastomers with strain greater than 100%*, Science, **287**, *5454*, pp. 836-839, 2000.
11. J.S. PLANTE, S. DUBOWSKY, *On the performance mechanisms of dielectric elastomer actuators*, Sensors and Actuators A: Physical, **137**, *1*, pp. 96-109, 2007.
12. C. KEPLINGER, T. LI, R. BAUMGARTNER, Z. SUO, S. BAUER, *Harnessing snap-through instability in soft dielectrics to achieve giant voltage-triggered deformation*, Soft Matter, **8**, *2*, pp. 285-288, 2012.
13. J. HUANG, S. SHIAN, R.M. DIEBOLD, Z. SUO, D.R. CLARKE, *The thickness and stretch dependence of the electrical breakdown strength of an acrylic dielectric elastomer*, Applied Physics Letters, **101**, *12*, p. 122905, 2012.
14. F. CARPI, S. BAUER, D. DE ROSSI, *Stretching dielectric elastomer performance*, Science, **330**, *6012*, pp. 1759-1761, 2010.
15. T. KASAHARA, M. MIZUSHIMA, H. SHINOHARA, T. OBATA, T. FUTAKUCHI, S. SHOJI, J. MIZUNO, *Simple and low-cost fabrication of flexible capacitive tactile sensors*, Japanese Journal of Applied Physics, **50**, *1R*, p. 016502, 2011.
16. D. KIM, C.H. LEE, B.C. KIM, D.H. LEE, H.S. LEE, C.T. NGUYEN, H.R. CHOI, *Six-axis capacitive force/torque sensor based on dielectric elastomer*, In: *Electroactive Polymer Actuators and Devices (EAPAD)*, Proceedings, Vol. 8687, p. 86872J, 2013.
17. F. CARPI, E. SMELA, *Biomedical applications of electroactive polymer actuators*, John Wiley & Sons, 2009.
18. R.D. KORNBLUH, R. PELRINE, H. PRAHLAD, A. WONG-FOY, B. MCCOY, S. KIM, T. LOW, *From boots to buoys: promises and challenges of dielectric elastomer energy harvesting*, In: *Electroactivity in polymeric materials* (ed. L. Rasmussen), Springer, 2012, pp. 67-93.
19. M. DUDUTA, D.R. CLARKE, R.J. WOOD, *A high speed soft robot based on dielectric elastomer actuators*, 2017 IEEE International Conference on Robotics and Automation (ICRA), pp. 4346-4351, 2017.
20. J. CAO, W. LIANG, Q. REN, U. GUPTA, F. CHEN, J. ZHU, *Modelling and control of a novel soft crawling robot based on a dielectric elastomer actuator*, IEEE International Conference on Robotics and Automation (ICRA), pp. 4188-4193, 2018.
21. F.A.M. GHAZALI, C.K. MAH, A. ABUZAITER, P.S. CHEE, M.S.M. ALI, *Soft dielectric elastomer actuator micropump*, Sensors and Actuators A: Physical, **263**, pp. 276-284, 2017.
22. J. ZOU, G. GU, *Modeling the viscoelastic hysteresis of dielectric elastomer actuators with a modified rate-dependent Prandtl-Ishlinskii model*, Polymers, **10**, *5*, p. 525, 2018.
23. A. SAINI, D. AHMAD, K. PATRA, *Electromechanical performance analysis of inflated dielectric elastomer membrane for micro pump applications*, In: *Electroactive Polymer Actuators and Devices (EAPAD)*, Vol. 9798, p. 979813, 2016.
24. H.F. BRINSON, L.C. BRINSON, *Polymer engineering science and viscoelasticity: An introduction*, Springer, 2008.
25. A.N. GENT, *Engineering with rubber: how to design rubber components*, 3rd edition, Carl Hanser Verlag GmbH Co KG, 2012.
26. M. SHAHZAD, A. KAMRAN, M.Z. SIDDIQUI, M. FARHAN, *Mechanical characterization and FE modelling of a hyperelastic material*, Materials Research, **18**, pp. 918-924, 2015.
27. O.H. YEOH, *Characterization of elastic properties of carbon-black-filled rubber vulcanizates*, Rubber chemistry and technology, **63**, *5*, pp. 792-805, 1990.
28. C. RENAUD, J.M. CROS, Z.Q. FENG, B. YANG, *The Yeoh model applied to the modeling of large deformation contact/impact problems*, International Journal of Impact Engineering, **36**, *5*, pp. 659-666, 2009.
29. P. LOCHMATTER, S.A. MICHEL, G.M. KOVACS, *Electromechanical model for static and dynamic activation of elementary dielectric elastomer actuators*, In: *Smart Structures and Materials 2006: Electroactive Polymer Actuators and Devices (EAPAD)*, Int. Soc. for Op. and Pht., Vol. 6168, p. 61680F, 2006.
30. E. YANG, M. FRECKER, E. MOCKENSTURM, *Finite element and experimental analyses of non-axisymmetric dielectric elastomer actuators*, In: *Smart Structures and Materials 2006: Electroactive Polymer Actuators and Devices (EAPAD)*, Vol. 6168, p. 61680H, 2006.
31. K., JUNG, J., LEE, M.S., CHO, J.C. KOO, Y.K. LEE, H.R. CHOI, *Development of enhanced synthetic rubber for energy efficient polymer actuators*, In: *Smart Structures and Materials 2006: Electroactive Polymer Actuators and Devices (EAPAD)*, Vol. 6168, p. 61680N, 2006.
32. A. O'HALLORAN, F. O'MALLEY, P. MCHUGH, *A review on dielectric elastomer actuators, technology, applications, and challenges*, Journal of Applied Physics, **104**, *7*, p. 9, 2008.
33. R. DELILLE, M. URDANETA, K. HSIEH, E. SMELA, *Novel compliant electrodes based on platinum salt reduction*. In: *Smart Structures and Materials 2006: Electroactive Polymer Actuators and Devices (EAPAD)*, Vol. 6168, p. 61681Q, 2006.
34. B. GUIFFARD, L. SEVEYRAT, G. SEBALD, D. GUYOMAR, *Enhanced electric field-induced strain in non-percolative carbon nanopowder/polyurethane composites*, Journal of Physics D: Applied Physics, **39**, *14*, p. 3053, 2006.
35. G.Y. GU, J. ZHU, L.M. ZHU, X. ZHU, *A survey on dielectric elastomer actuators for soft robots*, Bioinspiration & Biomimetics, **12**, *1*, p. 011003, 2017.
36. I. KARAMAN, D.E. ŞAHİN, *Experimental study on the variation of temperature in soft dielectric elastomer actuators*, Proceedings of the Romanian Academy, Series A: Mathematics Physics Technical Sciences Information Science, **22**, *3*, pp. 245-253, 2021.
37. Z. SUO, *Theory of dielectric elastomers*, Acta Mechanica Solida Sinica, **23**, *6*, pp. 549-578, 2010.